Novel metallo-dendrimers containing various Ru core ligands and dendritic thiophene arms for photovoltaic applications

ARTICLE · JUNE 2014

DOI: 10.1039/C4PY00444B

7 AUTHORS, INCLUDING:

Ramesh Mohan
National Chiao Tung University
14 PUBLICATIONS **63** CITATIONS
SEE PROFILE

Harihara Padhy
National Tsing Hua University
19 PUBLICATIONS **305** CITATIONS
SEE PROFILE

Kung-Hwa Wei
National Chiao Tung University
172 PUBLICATIONS **6,124** CITATIONS
SEE PROFILE

Hong-Cheu Lin
National Chiao Tung University
155 PUBLICATIONS **2,411** CITATIONS
SEE PROFILE

Polymer Chemistry

PAPER

View Article Online
View Journal | View Issue

Cite this: *Polym. Chem.*, 2014, **5**, 5423

Novel metallo-dendrimers containing various Ru core ligands and dendritic thiophene arms for photovoltaic applications

Rudrakanta Satapathy,[a] Mohan Ramesh,[a] Harihara Padhy,[a] I.-Hung Chiang,[a] Chih-Wei Chu,*[bc] Kung-Hwa Wei[a] and Hong-Cheu Lin*[a]

Received 28th March 2014
Accepted 22nd May 2014

DOI: 10.1039/c4py00444b

www.rsc.org/polymers

Three series of supramolecular mono-(*i.e.*, **Ru1G1**, **Ru1G2** and **Ru1G3**), bis-(*i.e.*, **BTRu2G1**, **BTRu2G2** and **BTRu2G3**) and tris-(*i.e.*, **TPARu3G1**, **TPARu3G2** and **TPARu3G3**) Ru-based dendritic complexes were synthesized. Their photophysical and electrochemical properties were investigated. These metallo-dendritic complexes covered a broad absorption range of 250–750 nm with optical bandgaps of 1.51–1.86 eV. The energy levels of the metallo-dendrimers can be effectively adjusted not only by different generations of dendritic thiophene arms but also by their π-conjugated core ligands bearing various electron donor (*i.e.*, triphenylamine) and acceptor (*i.e.*, benzothiadiazole) moieties. Due to the donor–acceptor effect, the bis-Ru-based dendrimers containing a benzothiadiazole electron-acceptor core ligand showed the highest power conversion efficiency (PCE) among these three series of metallo-dendrimers. The tris-Ru-based architecture with a triphenylamine electron-donor core ligand revealed moderate photovoltaic performance. Among the different generations (**G1–G3**) of dendrimers, the third generation (**G3**) possessed the highest PCE values in each series of Ru-based dendrimers. Hence, the third generation bis-'Ru'-based dendrimer **BTRu2G3** blended with $PC_{70}BM$ (1 : 3 w/w) showed the highest PCE value of 0.77% (without the aid of additives or annealing), which is the highest efficiency among all bulk hetero-junction (BHJ) solar cells containing metallo-dendrimers reported to date.

Introduction

The design of supramolecular assemblies possessing novel functional properties of tailored non-covalent structures are attracting increased interest in current research.[1] Especially, oligo-pyridyl ligands and their transition metal complexes have been developed for several applications such as active materials in self-assembled molecular devices, electroluminescent materials in molecular electronics and photonics, and luminescent sensor materials in molecular biology and medical diagnostics.[1] Directional and effective electron energy transfers could be achieved by the design of suitable multiple ligands and complexation with transition metal ions. Among the *N*-heterocyclic ligands, the remarkably high affinities of 2,2′:6′,2″-terpyridine towards transition-metal ions and chelation effects due to dπ–pπ* back-bonding of the metal ions to the pyridyl rings make them useful for supramolecular constructions. Compared with other transition metal ion complexes, due to the high binding strength of Ru(II) with the terpyridyl moiety, the Ru(II) complexes show remarkable stability and can only be cleaved under extreme conditions like low pH values, high temperatures and the addition of strong competitive ligands.[2] Suitable π-conjugated substituents at the 4′-position of the 2,2′:6′,2″-terpyridyl unit exhibit intriguing spectroscopic and redox properties, which cause effective electronic communications between the metal ions and π ligands.[3] Moreover, their photophysical, electrochemical and magnetic properties are strongly influenced by the nature of the π-conjugated moieties attached to the terpyridyl units.[3] Furthermore, the electronic communication between the metal-complexed terpyridines and the attached π-conjugated moieties are additionally fascinating features directing their potentials for the design of new supramolecular architectures. Recently, terpyridyl Ru(II) complexes have gained interest for the researchers to investigate their photovoltaic cell (PVC) applications.[4] Likewise, dyadic Ru(II) complexes consisting of 4′-substituted terpyridyl units have been utilized as specifically active candidates in organic photovoltaic cells.[5] These systems have received extensive attention owing to their very long-lived metal to ligand charge transfer (MLCT) excited states and high molar extinction coefficients in the visible range.[5] In these dyads, the excited state generated upon the absorption of light leads to a charge separated state with a high efficiency.[6] During the synthesis of dyadic polymers, large polydispersities and poor solubility

[a]*Department of Materials Science and Engineering, National Chiao Tung University, Hsinchu, Taiwan, ROC. E-mail: linhc@mail.nctu.edu.tw*

[b]*Research Center for Applied Sciences, Academia Sinica, Taipei, Taiwan, ROC. E-mail: gchu@gate.sinica.edu.tw*

[c]*Department of Photonics, National Chiao Tung University, Hsinchu, Taiwan, ROC*

might arise due to the various polymeric sizes (as well as molecular weights) and highly conjugated metallo-polymers, respectively, which could extensively amend the carrier mobilities of the OPV devices.[6a,b] Therefore, monodispersed materials are desirable to obtain efficient charge transports and device efficiencies in organic photovoltaic applications because of their aptitude to control the morphologies of the blends.[6c] In this respect, conjugated dendrimers offer an alternative to conjugated polymers to be useful in organic photovoltaics because of the following advantages. Dendrimers[6] (1) possess well-defined molecular weights with monodispersity; (2) have shape persistency, which allows them to maintain their structures in a solution-processable form; (3) can be synthesized with high purities compared with their polymeric derivatives; and (4) have their own internal local electric fields, which may be created during the charge transfer from the peripheral arms to the cores of dendrimers. In addition, conjugated dendrimers are expected to show a high degree of ordering in OPV devices due to their small size and monodisperse nature. To the best of our knowledge, however, there are only a few reports on the applications of dendrimers for organic solar cells.[7a–c] Metal-based supramolecular architectures for the development of bulk hetero-junction (BHJ) solar cells are under progress.[7d] Due to their three-dimensional hyper-branched structure, the branches become denser with increasing distance from the core, which produces shell effects on the dendrimers.[8] Thus, high-generation dendrimers possessing highly dense branches towards the outer surfaces may act as a barrier to restrict the charge transfer between the inner and outer parts of the dendrimers. Thiophene dendrimers and terpyridyl dendritic complexes have recently attained promising attention for the applications of photovoltaic and other optoelectronic applications.[8]

With the aim towards developing metallo-dendrimers for BHJ solar cell applications, mono-(*i.e.*, **Ru1G1**, **Ru1G2** and **Ru1G3**), bis-(*i.e.*, **BTRu2G1**, **BTRu2G2** and **BTRu2G3**) and tris-(*i.e.*, **TPARu3G1**, **TPARu3G2** and **TPARu3G3**) Ru-based dendritic complexes were prepared and characterized. We have compared their photophysical and photovoltaic properties in relation to their structural architecture.

Experimental section

Synthetic procedures

G1-SnBu$_3$. **G1** (2.1 g, 5.03 mmol) was dissolved in 25 mL THF and cooled to −78 °C. To this solution, 2.5 M *n*-BuLi in hexane (2.41 mL, 6.04 mmol) was added drop-wise. The reaction was stirred at −78 °C for 1 hour. To this solution, $SnBu_3Cl$ (1.96 g, 1.63 mL, 6.03 mmol) was added rapidly. The reaction mixture was allowed to warm to room temperature and then stirred overnight. The reaction mixture was quenched by the addition of 20 mL of H_2O, extracted with ethyl acetate and washed three times with water. The organic layer was dried over $MgSO_4$, and the solvent was removed by rotary evaporation to obtain the crude product as pale-yellow oil. The crude product was used for the next step without further purification. ^{1}H NMR ($CDCl_3$, 300 MHz): 7.10 (s, 1H), 6.91 (d, 1H, 3.3 Hz), 6.87 (d, 1H, 3.6 Hz), 6.66 (d, 2H, 3.3 Hz), 2.77 (m, 4H), 1.64 (m, 4H), 1.56 (m, 6H), 1.36 (t, 6H, 7.3 Hz), 1.30 (m, 12H), 1.11 (t, 6H, 8.3 Hz), 0.90 (m, 15H).

G1-TPY. **G1-SnBu$_3$** (3.5 g, 4.95 mmol), 4′-(5-bromo-4-dodecylthiophen-2-yl)-2,2′:6′,2″-terpyridine (1.62 g, 4.13 mmol) and $Pd(PPh_3)_4$ (114 mg, 0.099 mmol) was taken in a two-necked flask and degassed by nitrogen. Dry DMF (30 mL) was poured into this solution, and the reaction mixture heated to 90 °C overnight. Water (100 mL) was added to this solution, and the reaction mixture was extracted by EA. The organic layer was dried over $MgSO_4$ and the solvent was removed by rotary evaporation. The crude product was then purified by neutral alumina column chromatography using hexane : EA = 15 : 1 to yield pure compound (2.02 g, 67.1%). ^{1}H NMR ($CDCl_3$, 300 MHz): 8.75 (d, 2H, 6 Hz), 8.67 (s, 2H), 8.65 (d, 2H, 6 Hz), 7.90 (dt, 2H, 9 Hz, 1.2 Hz), 7.71 (1H, 3.9 Hz), 7.38 (2H, 6 Hz), 7.27 (s, 1H), 7.23 (d, 1H, 3 Hz), 6.98 (d, 1H, 3 Hz), 6.92 (d, 1H, 3 Hz), 6.69 (d, 2H, 3 Hz), 2.82 (t, 4H, 7.5 Hz), 1.70–1.61 (m, 4H), 1.39–1.26 (m, 12H), 0.94 (t, 6H, 6.5 Hz). ^{13}C NMR ($CDCl_3$, 300 MHz): 155.98, 155.88, 149.07, 147.73, 146.41, 142.80, 140.45, 138.32, 136.78, 134.58, 134.28, 132.44, 131.94, 131.11, 127.52, 126.67, 126.57, 126.41, 124.68, 124.23, 124.08, 123.85, 121.24, 116.56, 31.55, 31.52, 31.47, 28.74, 26.81, 22.57, 17.48, 14.07, 13.58 elemental analysis for $C_{43}H_{43}N_3S_4$: calculated: (%) C, 70.74; H, 5.94; N, 5.76. Found: (%) C, 70.29; H, 5.93; N, 5.90. MS (FAB): *m*/*z* 730 (calcd $(M)^+$: 730.08).

G2-SnBu$_3$. **G1** (1.8 g, 1.97 mmol) was dissolved in 25 mL THF and cooled to −78 °C. To this solution, 2.5 M *n*-BuLi in hexane (0.94 mL, 2.36 mmol) was added drop-wise. The reaction was stirred at −78 °C for 1 hour. To this solution. $SnBu_3Cl$ (0.83 g, 0.69 mL, 2.56 mmol) was added rapidly. The reaction mixture was then allowed to warm to room temperature and stirred overnight. The reaction mixture was quenched by the addition of 20 mL of H_2O, extracted with ethyl acetate and washed three times with water. The organic layer was dried over $MgSO_4$, and the solvent was removed by rotary evaporation to obtain the crude product as pale-yellow oil. The crude product was used for next step without further purification. ^{1}H NMR ($CDCl_3$, 300 MHz): 7.19 (s, 1H), 7.18 (s, 1H), 7.15 (s, 1H), 6.93 (t, 2H, 3 Hz), 6.87 (d, 2H, 3 Hz), 6.65 (m, 4H), 2.76 (t, 8H, 6.9 Hz), 1.69–1.57 (m, 14H), 1.36–1.29 (m, 30H), 1.11 (t, 6H, 8.2 Hz), 0.89 (m, 21H).

G2-TPY. **G$_2$-SnBu$_3$** (2.3 g, 1.91 mmol), 4′-(5-bromo-4-dodecylthiophen-2-yl)-2,2′:6′,2″-terpyridine (0.62 g, 1.59 mmol) and $Pd(PPh_3)_4$ (44 mg, 0.038 mmol) was taken in a two-necked flask and degassed by nitrogen. Dry DMF (25 mL) was poured into this solution, and the reaction mixture heated to 90 °C overnight. Water (100 mL) was added to this solution, and the reaction mixture was extracted with EA. The organic layer was dried over $MgSO_4$, and the solvent was removed by rotary evaporation. The crude product was purified by neutral alumina column chromatography using hexane : EA = 20 : 1 to yield pure compound (1.27 g, 54.2%). ^{1}H NMR ($CDCl_3$, 300 MHz): 8.75 (d, 2H, 6 Hz), 8.67 (s, 2H), 8.65 (d, 2H, 6 Hz), 7.90 (dt, 2H, 9 Hz, 1.2 Hz), 7.71 (1H, 3.9 Hz), 7.38 (2H, 6 Hz), 7.27 (s, 1H), 7.23 (d, 1H, 3 Hz), 6.98 (d, 1H, 3 Hz), 6.92 (d, 1H, 3 Hz) 6.69 (d, 2H, 3 Hz), 2.82 (t, 4H, 7.5 Hz), 1.70–1.61 (m, 4H), 1.39–1.26 (m, 12H), 0.94 (t, 6H, 6.5 Hz). ^{13}C NMR ($CDCl_3$, 300 MHz): 155.76, 155.72, 148.97, 147.62, 147.41146.27, 146.09142.43, 140.79, 137.65,

136.67, 135.61, 134.75, 134.48, 134.39, 132.19, 131.91, 131.87, 131.81, 130.24, 129.70, 127.59, 127.49, 126.51, 126.44, 126.26, 124.19, 124.05, 123.77, 121.16, 116.39, 116.20, 31.61, 31.51, 30.16, 28.82, 28.80, 27.83, 26.86, 25.60, 22.71, 22.63, 14.35, 13.64. Elemental analysis for $C_{71}H_{75}N_3S_8$: calculated: (%) C, 69.51; H, 6.16; N, 3.42. Found: (%) C, 69.32; H, 6.63; N, 3.41. MS (FAB): *m*/*z* 1227 (calcd $(M)^+$: 1226.90).

G3-SnBu$_3$. **G$_3$** (1.5 g, 0.78 mmol) was dissolved in 20 mL of THF and cooled to −78 °C. To this solution, 2.5 M *n*-BuLi in hexane (0.37 mL, 0.93 mmol) was added drop-wise. The reaction was stirred at −78 °C for 1 hour. To this solution, $SnBu_3Cl$ (0.33 g, 0.27 mL, 1.04 mmol) was added rapidly. The reaction mixture was then allowed to warm to room temperature and stirred overnight. Subsequently, the reaction mixture was quenched by the addition of 20 mL of H_2O, extracted with ethyl acetate and washed three times with water. The organic layer was dried over $MgSO_4$, and the solvent was removed by rotary evaporation to obtain the crude product as pale-yellow oil. The crude product was used for next step without further purification.

G3-TPY. **G$_2$-SnBu$_3$** (1.7 g, 0.77 mmol), 4′-(5-bromo-4-dodecylthiophen-2-yl)-2,2′:6′,2″-terpyridine (0.25 g, 0.64 mmol) and $Pd(PPh_3)_4$ (17.8 mg, 0.015 mmol) was taken into a two-necked flask and degassed with nitrogen. Dry DMF (15 mL) was poured into this solution, and the reaction mixture heated to 90 °C overnight. Water (100 mL) was added to this solution, and the reaction mixture was extracted with EA. The organic layer was dried over $MgSO_4$, and the solvent was removed by rotary evaporation. The crude product was purified by neutral alumina column chromatography using hexane : EA = 20 : 1 to yield pure compound (0.82 g, 48.2%). ^{1}H NMR ($CDCl_3$, 300 MHz): 8.72 (d, 2H, 6 Hz), 8.65 (s, 2H), 8.62 (d, 2H, 9 Hz), 7.77 (t, 2H, 9 Hz), 7.59 (d, 3 Hz), 7.29–7.24 (m, 7H), 7.18 (s, 1H), 7.12 (d, 1H, 2.7 Hz), 7.02 (s, 1H), 6.97 (m, 4H), 6.91 (m, 4H), 6.65 (m, 8H), 2.74 (t, 16H, 7.4 Hz), 1.63 (m, 16H), 1.34 (m, 48H), 0.96 (t, 24H, 5.4 Hz). ^{13}C NMR ($CDCl_3$, 300 MHz): 155.98, 155.82, 149.06, 147.60, 147.35, 147.29, 146.23, 146.19, 146.06, 146.02, 142.66, 141.13, 137.65, 136.79, 136.11, 135.30, 134.76, 134.46, 134.42, 134.36, 133.17, 133.08, 132.95, 132.58, 132.31, 132.21, 132.16, 131.95, 131.86, 131.72, 131.37, 131.31, 130.47, 130.39, 130.26, 129.73, 129.59, 127.64, 127.52, 126.66, 126.43, 126.39, 126.25, 125.26, 124.10, 123.94, 121.25, 116.65, 31.54, 31.46, 30.14, 30.10, 28.77, 22.57, 14.05. Elemental analysis for $C_{127}H_{139}N_3S_{16}$: calculated: (%) C, 68.69; H, 6.31; N, 1.89. Found: (%) C, 67.86; H, 6.75; N, 1.73. MS (MALDI-TOF): *m*/*z* 2220.7 (calcd $(M)^+$: 2220.52) .

G1-TPY-RuCl$_3$. **G1-TPY** (600 mg, 0.822 mmol) and **RuCl$_3$**·*x*H_2O (236.46 mg, 0.906 mmol) were taken in MeOH : THF/5 : 1 under a N_2 atmosphere, and then the mixture was refluxed overnight. The solid residue was filtered, washed with an excess of methanol and dried to obtain the product as a shiny black solid (746.04 mg, 97%).

G2-TPY-RuCl$_3$. **G2-TPY** (500 mg, 0.407 mmol) and **RuCl$_3$**·*x*H_2O (117 mg, 0.448 mmol) were taken in MeOH : THF/5 : 1 (100 mL) under a N_2 atmosphere, and the mixture was refluxed overnight. The solid residue was filtered, washed with an excess of methanol and dried to obtain the product as a black solid (574.28 mg, 98.5%).

G3-TPY-RuCl$_3$. **G3-TPY** (400 mg, 0.18 mmol) and **RuCl$_3$**·*x*H_2O (51.15 mg, 0.196 mmol) were taken in MeOH : THF/5 : 1 (100 mL) under a N_2 atmosphere, and the mixture was refluxed overnight. The solid residue was filtered, washed with an excess of methanol and dried to obtain the product as a black solid (420.52 mg, 96.4%).

Ru1G1. **G1-TPY-RuCl$_3$** (360 mg, 0.385 mmol) and $AgBF_4$ (300 mg, 1.54 mmol) were taken in acetone (60 mL) and refluxed for 18 hours under a N_2 atmosphere. The solution was filtered to remove the AgCl salt. The filtrate was evaporated, and to the residue, **G1-TPY** (280 mg, 0.385 mmol) was added. The mixture was then dissolved in 5 mL of dimethyl acetamide and 50 mL of *n*-BuOH, and refluxed for 24 hours. The reaction mixture obtained was cooled and added drop-wise into a beaker containing 500 mL MeOH with stirring. The solid was then filtered, washed with MeOH and a 5 : 1 mixture of MeOH : acetone. The residue was dried to obtain a dark red solid (560.04 mg, 93.2%). ^{1}H NMR (DMSO-d_6, 300 MHz): 9.33 (s, 4H), 9.11 (d, 4H, 8.1 Hz), 8.48 (d, 2H, 3.9 Hz), 8.07 (t, 4H, 7.5 Hz), 7.82 (d, 2H, 3.6 Hz), 7.72 (s, 2H), 7.60 (d, 4H, 6 Hz), 7.28 (t, 4H, 6.2 Hz), 7.12 (d, 4H, 3.6 Hz), 6.87 (d, 2H, 3.6 Hz), 6.85 (d, 2H, 3.3 Hz), 2.78 (t, 8H, 7.5 Hz), 1.60–1.57 (m, 8H), 1.35–1.24 (m, 24H), 0.86 (t, 12H, 6.6 Hz). Elemental analysis for $C_{86}H_{86}N_6RuS_8$: calculated: C, 66.16; H, 5.55; N, 5.38. Found: (%) C, 66.86; H, 5.75; N, 5.43. MS (MALDI-TOF): *m*/*z* 1559.24, (calcd $(M)^+$: 1560.37).

Ru1G2. **G2-TPY-RuCl$_3$** (340 mg, 0.237 mmol) and $AgBF_4$ (194.67 mg, 0.949 mmol) were taken in acetone (50 mL) and refluxed for 20 hours under a N_2 atmosphere. The solution was filtered to remove the AgCl salt. The filtrate was evaporated, and to the residue, **G2-TPY** (290.3 mg, 0.237 mmol) was added. The mixture was then dissolved in 5 mL of dimethyl acetamide and 50 mL of *n*-BuOH, and refluxed for 24 hours. The reaction mixture obtained was cooled and added drop-wise into a beaker containing 500 mL of MeOH with stirring. The solid was filtered, washed with MeOH and a 6 : 1 mixture of MeOH : acetone. The residue was then dried to obtain a dark red solid (559.77 mg, 94.1%). ^{1}H NMR (DMSO-d_6, 300 MHz): 9.35–9.28 (br, 4H), 9.11 (d, 4H, 8.1 Hz), 8.50–8.43 (br, 2H), 8.07 (br, 4H), 7.90–7.83 (br, 4H), 7.58–7.49 (br, 10H), 7.38–7.28 (br, 4H), 7.05–7.02 (br, 8H), 6.82–6.78 (br, 8H), 2.77–2.74 (br, 16H), 1.57–1.55 (br, 16H), 1.27 (br, 48H), 0.85 (br, 24H). Elemental analysis for $C_{142}H_{150}N_6RuS_{16}$: calculated: C, 66.76; H, 5.92; N, 3.29. Found: (%) C, 66.16; H, 5.25; N, 3.73. MS (MALDI-TOF): *m*/*z* 2554.58, (calcd $(M)^+$: 2553.65).

Ru1G3. **G3-TPY-RuCl$_3$** (7.2 mg, 0.18 mmol) and $AgBF_4$ (140 mg, 0.721 mmol) were taken in acetone (50 mL) and refluxed for 20 hours under a N_2 atmosphere. The solution was then filtered to remove the AgCl salt. The filtrate was evaporated, and to this residue, **G3-TPY** (400 mg, 0.18 mmol) was added. The mixture was then dissolved in 5 mL of dimethyl acetamide and 50 mL of *n*-BuOH, and refluxed for 24 hours. The reaction mixture obtained was cooled and added drop-wise into a beaker containing 500 mL of MeOH with stirring. The solid was filtered, washed with MeOH and a 6 : 1 mixture of MeOH : acetone. The residue was dried to obtain a dark red solid (749.72 mg, 91.7%). ^{1}H NMR ($CDCl_3$, 300 MHz): 8.85 (br, 4H), 8.70–8.62 (br, 4H),

8.16 (br, 2H), 7.86 (br, 4H), 7.41 (br, 4H), 7.24–7.05 (br, 20H), 6.90–6.82 (br, 16H), 6.61–6.57 (br, 16H), 2.73–2.69 (br, 32H), 1.65–1.58 (br, 32H), 1.26 (br, 96H), 0.85 (br, 48H). Elemental analysis for $C_{254}H_{278}N_6RuS_{32}$: calculated: C, 67.17; H, 6.17; N, 1.85. Found: (%) C, 66.16; H, 5.25; N, 3.73. MS (MALDI-TOF): *m*/*z* 4537.05, (calcd $(M)^+$: 4541.21).

Synthesis of the core ligand for the double metal system. The core ligand for the double metal system was prepared by our previously reported procedure.[5c]

General synthetic procedure of double metal systems. G-TPY-RuCl$_3$ (2.1 equiv. w.r.t. **BT2TPY**) and $AgBF_4$ (6.4 equiv. w.r.t. **TPA3TPY**) were taken in acetone (50 mL) and refluxed 36 h under a N_2 atmosphere. The solution was filtered to remove the AgCl salt. The filtrate was evaporated, and to the residue, **BT2TPY** (1 equiv.) was added. The mixture was then dissolved in 5 mL of dimethyl acetamide and 50 mL of *n*-BuOH, and refluxed for 48 hours. The reaction mixture obtained was cooled and added drop-wise into a beaker containing 500 mL MeOH with stirring. The solid was filtered, washed in MeOH and a 6 : 1 mixture of MeOH : acetone. The residue was then dried and recrystallized from a mixture of acetone : MeOH (1 : 10) to obtain the desired compounds.

BTRu2G1. Black powder. Yield: 59.6%. ^{1}H NMR (DMSO-d_6, 300 MHz): 9.37–9.35 (br, 8H), 9.10 (br, 8H), 8.56–8.47 (m, br, 8H), 8.39–8.32 (m, br, 8H), 8.23–8.07 (m, br, 8H), 7.93–7.68 (m, br, 6H), 7.59–7.47 (m, br, 6H), 7.28 (s, br, 2H), 7.19–7.10 (m, br, 4H), 6.86–6.64 (m, br,4H), 2.76–2.62 (m, br, 12H), 1.54–1.42 (m, br, 12H), 1.32–1.20 (m, br, 36H), 0.90–0.81 (m, br, 18H). MS (MALDI-TOF): *m*/*z* 2756.15 (calcd $(M)^+$: 2757.59).

BTRu2G2. Black powder. Yield: 55.2%. ^{1}H NMR (DMSO-d_6, 300 MHz): 9.35 (br, 8H), 9.10 (br, 8H), 8.52–8.49 (m, br, 8H), 8.32–8.23 (m, br, 8H), 8.07 (m, br, 8H), 7.92–7.89 (m, br, 6H), 7.75–7.48 (m, br, 7H), 7.40–7.28 (m, br, 5H), 7.04–7.02 (m, br, 8H), 6.87–6.78 (m, br, 8H), 2.76–2.71 (m, br, 20H), 1.58–1.42 (m, br, 20H), 1.25–1.19 (m, br, 60H), 0.85–0.76 (m, br, 30H). MS (MALDI-TOF): *m*/*z* 3752.55 (calcd $(M)^+$: 3751.87).

BTRu2G3. Black powder. Yield: 51.3%. ^{1}H NMR (DMSO-d_6, 300 MHz): 9.35–9.24 (br, 8H), 9.11 (br, 8H), 8.76–8.63 (m, br, 8H), 8.49–8.22 (m, br, 8H), 8.06–8.00 (m, br, 8H), 7.86–7.51 (m, br, 14H), 7.53–7.29 (m, br, 12H), 7.01–6.87 (m, br, 16H), 6.66 (m, br, 16H), 2.77–2.73 (m, br, 36H), 1.57–1.41 (m, br, 36H), 1.27–1.25 (m, br, 108H), 0.84–0.72 (m, br, 54H). MS (MALDI-TOF): *m*/*z* 5735.05 (calcd $(M)^+$: 5738.42).

Synthesis of the core ligand for the triple metal system. 2-Bromo-3-dodecylthiophene. 3-Hexylthiophene (5.2 g, 20.59 mmol) was dissolved in 250 mL of THF and cooled in an ice bath. NBS (3.66 g, 20.59 mmol) was added in one portion. Stirring was continued in the ice bath for 1 h and the mixture was poured into water. The organic layer was then extracted with hexanes two times (50 mL × 2) and then dried over $MgSO_4$. The solvent was removed under reduced pressure, and the crude oil obtained was purified by column chromatography on silica gel to afford 6.47 g of compound (94.9%). ^{1}H NMR ($CDCl_3$, 300 MHz): 7.19 (d, 1H, 5.6 Hz), 6.80 (d, 1H, 5.6 Hz), 2.55 (t, 2H, 7.5 Hz), 1.59–1.54 (m, 2H), 1.29–1.25 (m, 18H), 0.88 (t, 3H, 6.3 Hz).

5-Bromo-4-dodecylthiophene-2-carbaldehyde. To a mixture of *N*,*N*-dimethylformamide (27.27 g, 0.37 mol) and 30 mL of 1,2-dichloroethane at 0 °C, phosphorus oxychloride (47.26 g, 0.30 mol) was added drop-wise. Then, the mixture was heated to 35 °C and 2-bromo-3-dodecylthiophene (6.02 g, 0.018 mol) was added. After stirring for 24 h at 90 °C, the mixture was poured into 300 mL of water, and then extracted with chloroform. The organic phase was washed with water repeatedly and dried over $MgSO_4$. Finally, the solvent was removed and the residue purified by column chromatography (EA : hexane = 5 : 95) to obtain an orange liquid (4.82 g, 74.6%). ^{1}H NMR ($CDCl_3$, 300 MHz): 9.74 (s, 1H), 7.48 (s, 1H), 2.59 (t, 1H, 7.5 Hz), 1.62–1.57 (m, 2H), 1.31–1.25 (m, 18H), 0.87 (t, 3H, 6.6 Hz).

4′-(5-Bromo-4-dodecylthiophen-2-yl)-2,2′:6′,2″-terpyridine. To a solution of 2-acetyl pyridine (3.79 g, 3.51 mL, 31.3 mmol) in methanol (50 mL), an aqueous solution of sodium hydroxide (3.5 g, 87.5 mmol in 20 mL water) was added drop-wise. The reaction mixture was then stirred for 30 min. Then, 5-bromo-4-dodecylthiophene-2-carbaldehyde (4.5 g, 12.52 mmol) in 50 mL of methanol was added drop-wise, and the reaction mixture was stirred at room temperature for 18 hours. Finally, the solvent was evaporated, and the crude product was extracted from water with dichloromethane. To the above crude product an excess of ammonium acetate (35 g) in 150 mL of acetic acid–ethanol (2 : 1) was added. The reaction mixture was heated at reflux for 30 hours, and the mixture was cooled and poured into 500 mL water. The organic phase was extracted with dichloromethane, dried over $MgSO_4$ and the solvent was removed by rotary evaporation. The crude product was purified by neutral alumina column chromatography (DCM–hexane = 20 : 80) to obtain the pure product as a yellow solid (3 g, 42.5%). ^{1}H NMR ($CDCl_3$, 300 MHz): 8.73 (d, 2H, 4.8 Hz), 8.64 (d, 2H, 8.1 Hz), 7.87 (t, 2H, 7.6 Hz), 7.48 (s, 1H), 7.35 (m, 2H), 2.60 (t, 2H, 7.6 Hz), 1.64–1.60 (m, 2H), 1.34–1.25 (m, 18H), 0.86 (t, 3H, 6.9 Hz). ^{13}C NMR ($CDCl_3$, 300 MHz): 156.53, 156.30, 149.53, 143.99, 143.15, 141.40, 137.29, 127.06, 124.37, 121.73, 116.83, 111.54, 32.32, 30.13, 30.08, 29.97, 29.67, 23.09, 14.53. Elemental analysis for $C_{31}H_{36}BrN_3S$: calculated: (%) C, 66.18; H, 6.45; N, 7.47. Found: (%)C, 66.57; H, 6.02; N, 7.15. MS (FAB) *m*/*z* 561.10 (calcd $(M)^+$: 561.18).

Tris(4-(4,4,5,5-tetramethyl-1,3,2-dioxaborolan-2-yl)phenyl)-amine:.[8i] ^{1}H NMR ($CDCl_3$, 300 MHz): 7.69 (d, 6H, 8.4 Hz), 7.08 (d, 6H, 8.5 Hz), 1.33 (s, 36H).

TPA3TPY. In a 100 mL flame-dried two-necked flask fitted with a condenser, tris(4-(4,4,5,5-tetramethyl-1,3,2-dioxaborolan-2-yl)phenyl)amine (0.6 g, 0.96 mmol), 4′-(5-bromo-4-dodecylthiophen-2-yl)-2,2′:6′,2″-terpyridine (2 g, 3.55 mmol) and tetrakis(triphenylphosphine)palladium (55.65 mg, 0.048 mmol) was added. The mixture was degassed and purged with nitrogen. Then, 40 mL of anhydrous toluene and 2 M aqueous potassium carbonate solution (8 mL) was added. The reaction mixture was heated to 90 °C with vigorous stirring until the reaction completion, which was confirmed by TLC analysis (~55 hours). Then, the mixture was poured into water (100 mL) and extracted with dichloromethane. The organic layer was washed thrice with water, once with brine and dried over $MgSO_4$. The solvent was evaporated and the residue purified by neutral alumina column chromatography (DCM : hexane = 60 : 40) to obtain the pure product as a yellow solid (1.17 g, 75.5%). ^{1}H NMR ($CDCl_3$,

300 MHz): 8.76 (d, 6H, 4.7 Hz), 8.68 (s, 6H), 8.67 (d, 6H, 7.9 Hz), 7.88 (t, 6H, 7.6 Hz), 7.69 (s, 3H), 7.48 (d, 6H, 7.4 Hz), 7.38 (t, 6H, 7.8 Hz), 7.29 (s, 6H), 2.76 (t, 6H, 7.14 Hz), 1.73–1.65 (m, 6H), 1.41–1.23 (m, 54H), 0.84 (t, 9H, 6.3 Hz). ^{13}C NMR ($CDCl_3$, 300 MHz): 156.08, 155.91, 149.07, 146.61, 143.39, 139.78, 139.66, 138.85, 136.81, 133.11, 132.11, 131.98, 131.93, 130.04, 129.05, 128.54, 128.49, 128.38, 124.16, 123.82, 121.29, 116.52, 31.87, 3.06, 29.68, 29.62, 29.51, 29.34, 29.09, 22.65, 14.09. Elemental analysis for $C_{111}H_{120}N_{10}S_3$: calculated: (%) C, 78.87; H, 7.16; N, 8.29. Found: (%) C, 79.15; H, 7.62; N, 8.53. MS (MALDI-TOF): *m*/*z* 1690.08 (calcd $(M)^+$: 1690.40).

General procedure for the synthesis of the triple metal system. G-TPY-RuCl$_3$ (3.2 equiv. w.r.t. **TPA3TPY**) and $AgBF_4$ (12.8 equiv. w.r.t. **TPA3TPY**) were taken in acetone (50 mL) and refluxed for 36 hours under a N_2 atmosphere. The solution was filtered to remove the AgCl salt. The filtrate was evaporated, and to the residue, **TPA3TPY** (1 equiv.) was added. The mixture was dissolved in 5–7 mL dimethyl acetamide and 50 mL of *n*-BuOH, and refluxed for 48 hours. The product was cooled and added drop-wise into a beaker containing 500 mL of MeOH with stirring. The solid was filtered, washed with MeOH and a 6 : 1 mixture of MeOH : acetone. Finally, the residue was dried and recrystallized from a mixture of acetone : MeOH (1 : 10) to obtain the desired compounds.

TPARu3G1. Black powder. Yield: 69%. ^{1}H NMR (DMSO-d_6, 300 MHz): 9.31–9.27 (m, br, 12H), 9.08 (m, br, 12H), 8.77 (s, br, 3H), 8. 66 (s, br, 3H), 8.20–7.86 (m, br, 15H), 7.84 (s, br, 3H), 7.65–7.56 (m, br, 18H), 7.27 (br, 18H), 7.11 (m, br, 6H), 6.88 (m, br, 6H), 2.75–2.70 (m, br, 18H), 1.57–1.47 (m, br, 18H), 1.20 (m, br, 90H), 0.82–0.73 (m, br, 27H). MS (MALDI-TOF): *m*/*z* 4186.25 (calcd $(M)^+$: 4184.31).

TPARu3G2. Black powder. Yield: 61%. ^{1}H NMR (DMSO-d_6, 300 MHz): 9.34 (m, br, 12H), 9.10–9.07 (m, br, 12H), 8.49 (m, br, 6H), 8.06 (m, br, 12H), 7.89 (m, br, 12H), 7.59–7.48 (m, br, 24H), 7.38–7.28 (m, br, 12H), 7.04–7.02 (m, br, 12H), 6.81–6.78 (m, br, 12H), 2.75–2.73 (m, br, 30H), 1.56–1.44 (m, br, 30H), 1.26–1.21 (m, br, 126H), 0.84–0.78 (m, br, 45H). MS (MALDI-TOF): *m*/*z* 5670.24 (calcd $(M)^+$: 5673.73).

TPARu3G3. Black powder. Yield: 54%. ^{1}H NMR ($CDCl_3$, 300 MHz): 8.83 (br, 12H), 8.61 (br, 12H), 8.16 (br, 6H), 7.84 (br, 12H), 7.62–7.26 (br, 24H), 7.25–7.15 (br, 42H), 6.90 (br, 24H), 6.64 (br, 24H), 2.74 (br, 54H), 1.62 (br, 54H), 1.31–1.25 (br, 246H), 0.87 (br, 33H). MS (MALDI-TOF): *m*/*z* 8660.24 (calcd $(M)^+$: 8655.18).

Results and discussion

Materials and instrumentation

All chemicals and solvents were of reagent grade and purchased from Aldrich, ACROS, Fluka, TCI, TEDIA and Lancaster Chemical Co. Toluene, tetrahydrofuran and diethyl ether were distilled over sodium/benzophenone to make the solvents anhydrous before use. Chloroform ($CHCl_3$) was purified by refluxing with calcium hydride and then distilled. If not otherwise specified, solvents were degassed with nitrogen 1 h prior to use. Synthesis of 2-(4-hexylthiophen-2-yl)-4,4,5,5-tetramethyl-1,3,2-dioxaborolane and 4,7-dibromo-2,1,3-benzothiadiazole was performed by following previously reported procedures.

^{1}H NMR spectra were recorded on a Bruker DX-300 (300 MHz) spectrometer using $CDCl_3$ and DMSO-d_6 as solvents. Elemental analyses were performed on a HERAEUS CHN-OS RAPID elemental analyzer. UV-visible absorption spectra were recorded in dilute chloroform solutions (10^{-6} M) on a HP G1103A spectrophotometer. Solid films for UV-vis measurements were spin-coated on quartz substrates from chloroform solutions with a concentration of 10 mg mL^{-1}. Cyclic voltammetry (CV) measurements were performed using a BAS 100 electrochemical analyzer with a standard three-electrode electrochemical cell in a 0.1 M tetrabutylammonium hexafluorophosphate (Bu_4NPF_6) solution in (acetonitrile) at room temperature with a scanning rate of 100 mV s^{-1}. During the CV measurements, the solutions were purged with nitrogen for 30 s. In each case, a carbon working electrode coated with a thin layer of monomers or polymers, a platinum wire as the counter electrode and a silver wire as the quasi-reference electrode were used, and a Ag/AgCl (3 M KCl) electrode served as a reference electrode for all potentials quoted herein. The redox couple of ferrocene/ferrocenium ion (Fc/Fc^+) was used as an external standard. The corresponding HOMO and LUMO levels were calculated using $E_{ox/onset}$ and $E_{red/onset}$ for the experiments in solid films, which were performed by drop-casting films with similar thicknesses from $CHCl_3$ solutions (*ca.* 5 mg mL^{-1}).

Synthesis and structural characterization

Schematic representations and final chemical structures of the mono-, bis- and tris-Ru-based systems are depicted in Fig. 1–4, respectively. Three generations of thiophene dendrimers (**G1**, **G2** and **G3**) were synthesized.[8f] As shown in Scheme 1, a Stille coupling of 4′-(2-bromo-5-thienyl)-2,2′,6′,2″-terpyridine with **G1-SnBu$_3$**, **G2-SnBu$_3$** and **G3-SnBu$_3$** produced **G1-TPY**, **G2-TPY** and **G3-TPY**, respectively. The single metal system, *i.e.*, **Ru1G1**, **Ru1G2** and **Ru1G3**, were prepared according to Scheme 2. The core ligand of the double metal system was prepared following Scheme 3. The synthetic route for the preparation of the core ligand in the triple metal system is depicted in Scheme 4. The good solubilities of all central core ligands and dendritic metal complexes in common organic solvents, such as DCM, THF, EA, DMF and DMA, resulted in easy processibility during device fabrication. The chemical structures of the metallo-dendritic complexes and their ligands were confirmed by NMR, Maldi-TOF and UV-Vis characterization. As illustrated in the NMR spectra shown in Fig. 5, the clear and drastic downfield shifts of the (3,3″)- and (3′,5′)-terpyridyl signals, along with upfield shifts for the (6,6″)-terpyridyl signals were observed upon complexation with the Ru metals. In Fig. 6, the peaks at *ca.* 550 nm of the UV-vis spectra, which depicted a metal to ligand charge transfer (MLCT) peak, further confirmed the complexation of Ru in the metallo-dendritic architecture. Maldi-TOF mass spectra further verified the formation of the desired dendritic metal complexes.

Optical and electrochemical properties

The photophysical properties of the mono-, bis- and tris-Ru-based dendritic complexes were investigated by UV-vis absorption spectroscopy in both dilute solutions (10^{-6} M) and spin-

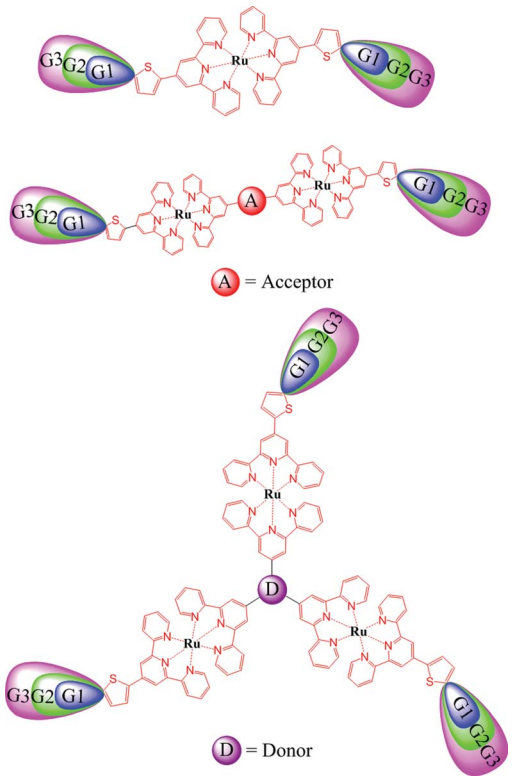

Fig. 1 Schematic representations of the mono-, bis- and tris-Ru-based systems.

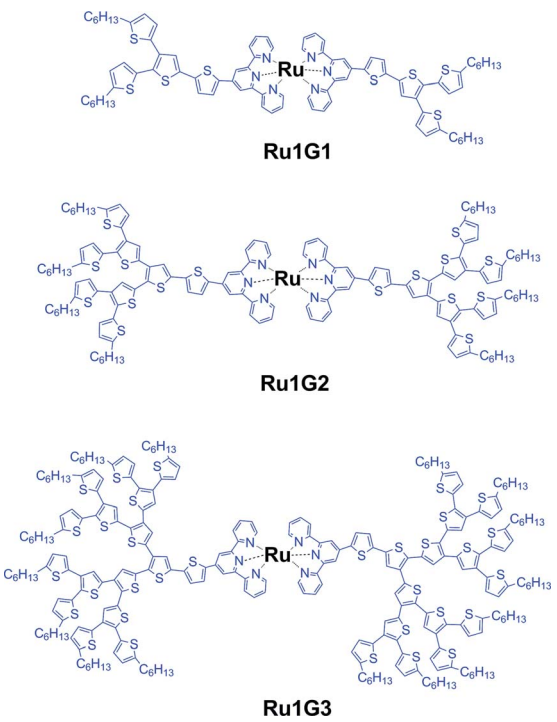

Fig. 2 Chemical structures of the supramolecular mono-Ru-based systems (**Ru1G1**, **Ru1G2** and **Ru1G3**).

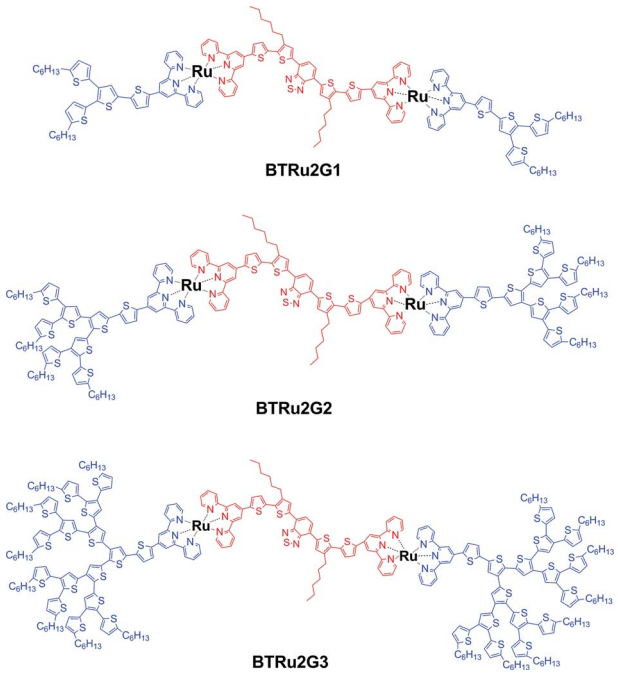

Fig. 3 Chemical structures of the supramolecular bis-Ru-based systems (**BTRu2G1**, **BTRu2G2** and **BTRu2G3**).

coated solid films on quartz substrates. Their absorption wavelengths (λ_{abs}), optical bandgaps (E_g^{opt}) and absorption onsets (λ_{onset}) in both solutions and film states are summarized in Table 1, where the metallo-dendrimers covered a broad absorption range of 250–750 nm with optical bandgaps of 1.51–1.86 eV. Fig. 6a shows the absorption spectra of the single metal system (**Ru1G1**, **Ru1G2** and **Ru1G3**) in both solution and film states. The peaks at ~300 nm correspond to the π–π* transitions of the terpyridyl moieties. Peaks at ~400 nm evolve from the π–π* transitions in the π-conjugated thiophene dendritic arms. In these Ru(II)-based metallo-dendrimers, self-assembly induced by the metal ions was readily observed by the occurrence of an additional absorption band, corresponding to a metal-to-ligand charge transfer (MLCT) ranging from 500–580 nm, which resulted from the promotion of an electron from the metal (Ru^{II})-centered d-orbital to the unfilled ligand-centered π* orbitals. Peaks at ~550 nm arise from the MLCT of the dendritic metal complexes. Fig. 6b shows the absorption spectra of the double metal system (**BTRu2G1**, **BTRu2G2** and **BTRu2G3**) in both solution and film states. In the film state, the MLCT peaks at ~550 nm were significantly shifted bathochromically with the concomitant shifts in the absorption onsets. This was attributed to the enhancement of the π–π* stacking by aggregation of the neighboring dendritic supramolecular partners in the solid state. Fig. 6c depicts the absorption spectra of the triple metal system (**TPARu3G1**, **TPARu3G2** and **TPARu3G3**) in both solution and film states. Like the double metal system, the MLCT peaks of the tris-Ru-based dendritic complexes at ~550 nm were shifted bathochromically with notable shifts in the absorption onsets, which corresponded to the strong intramolecular associations

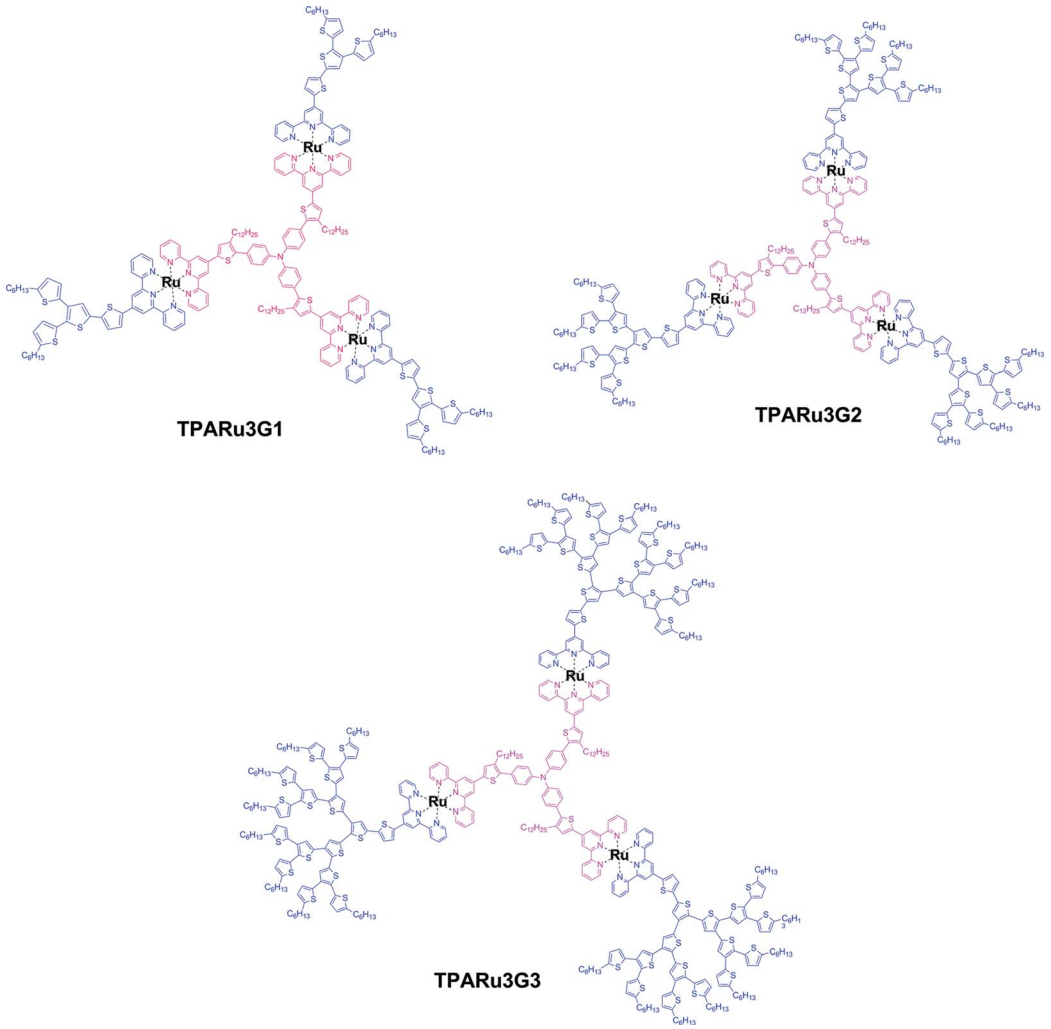

Fig. 4 Chemical structures of the supramolecular tris-Ru-based systems (TPARu3G1, TPARu3G2 and TPARu3G3).

and aggregations in the solid film. It is worthy to mention that the absorption of these Ru-based dendritic complexes showed extended absorptions beyond their MLCT peaks. Due to the extended absorptions, these metallo-dendritic complexes possessed small optical bandgaps (1.51–1.86 eV). The optical band gaps showed decreasing trends as the dendrimers' generation increased (G1–G3) among the three systems of metallo-dendritic complexes. The double metal system revealed lower optical bandgaps than the other systems (*i.e.*, single and triple metal systems). This can be attributed to the donor–acceptor architecture in the double metal system (*i.e.*, **BTRu2G1**, **BTRu2G2**, and **BTRu2G3**), which possess an electron acceptor unit in the benzothiadiazole core ligand that caused an efficient intramolecular electron transfer.

We further investigated the time-resolved fluorescence measurements for the three systems of metallo-dendritic complexes probed at 510 nm (excited at 375 nm). The time resolved lifetime spectra of the metallo-dendritic complexes are depicted in Fig. 7. A single exponential fitting for the fluorescence lifetime of the metallo-dendritic complexes, corresponding to the lifetime of the S1 state, are also summarized in Table 1. All these metallo-dendritic complexes showed very diminutive fluorescence lifetime values. However, the fluorescence lifetime values of the single and double metal systems were found to be the largest and smallest, respectively, among the three systems of metallo-dendritic complexes. The lifetime values of the double metal system were found to be smallest and the triple metal system showed moderate fluorescence lifetime values. Moreover, it was also observed that the fluorescence lifetime values decreased gradually with the higher generations of the metallo-dendritic complexes from G1 to G3.

To determine the electronic properties of the three series of metallo-dendritic complexes, the HOMO and LUMO levels were investigated by CV measurements in the solid films with Ag/AgCl as a reference electrode, calibrated by ferrocene ($E_{1/2(\text{ferrocene})} = 0.45$ mV *vs.* Ag/AgCl). The CV voltammograms are depicted in Fig. 8 and the energy levels are summarized in Table 2. The HOMO and LUMO levels were estimated by the oxidation and reduction potentials from the reference energy level of ferrocene (4.8 eV below the vacuum level) according to the following equation: $E_{\text{HOMO/LUMO}} = [-(E_{\text{onset}} - 0.45) - 4.8]$ eV. With an increase in the generations of the dendritic metal

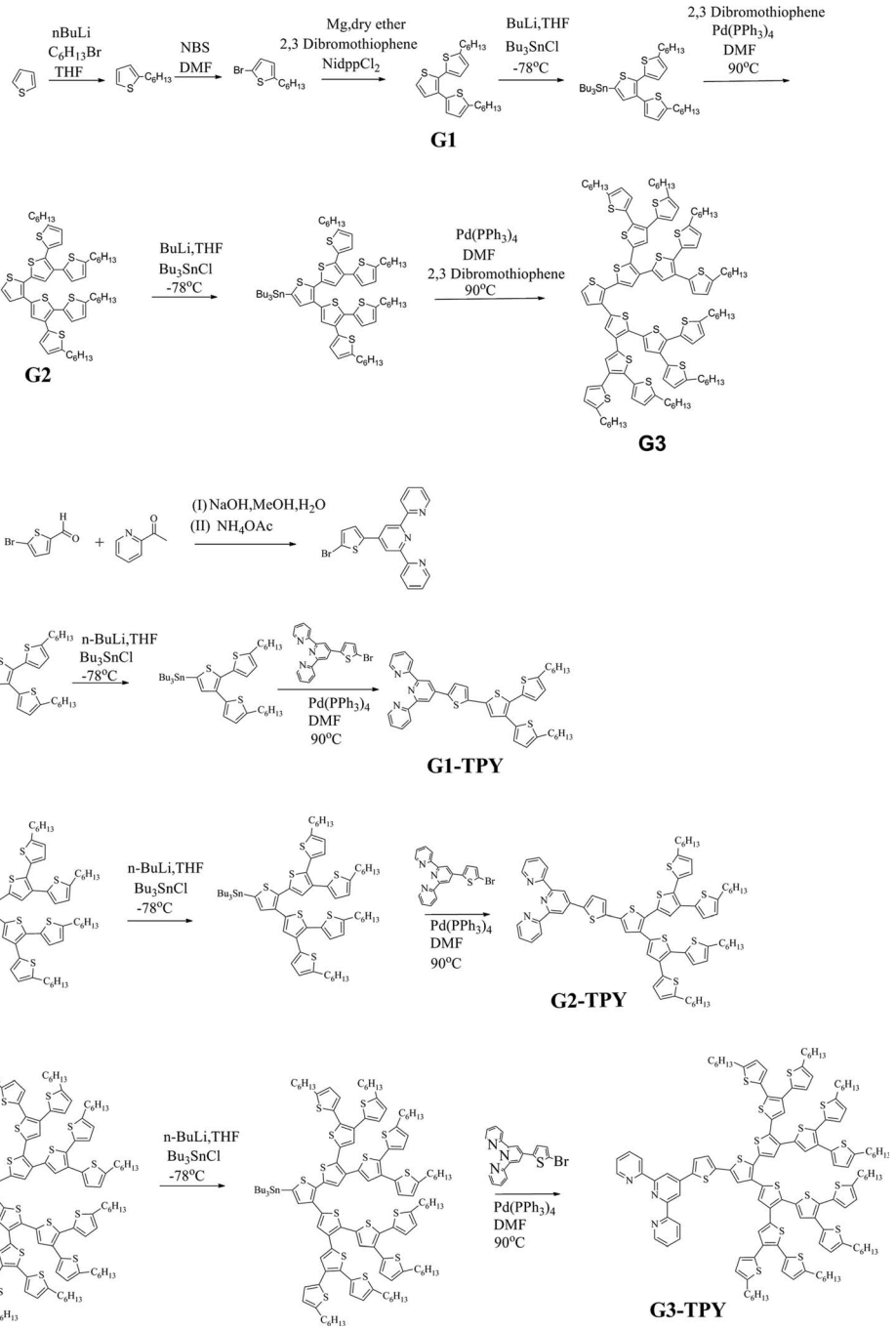

Scheme 1 Synthetic procedures for the different generations of the terpyridyl dendritic arms.

complexes, the electron donating ability of metallo-dendritic complexes increased, which resulted in the subsequent increases of the HOMO levels in each series of the metallo-dendritic complexes. The relatively low bandgaps of the double metal system were due to the donor–acceptor architecture of the benzothiadiazole core as an electron acceptor and the thiophene dendritic arms as electron donors. Although there are some deviations in the optical and electrochemical bandgaps, the trend of the bandgaps in the three series of metallo-dendritic complexes is similar.

Device fabrication and photovoltaic properties

To investigate the potential applications of the mono-, bis- and tris-Ru(II)-based dendritic complexes in PVCs, the BHJ solar cell devices, comprising an active layer of metallo-dendritic complexes as electron donors, blended with **$PC_{70}BM$** as an electron acceptor were fabricated with a configuration of ITO/PEDOT:PSS(30 nm)/metallo-dendritic complexes:**$PC_{70}BM$** = 1 : 1 (w/w) (~80 nm)/Ca(30 nm)/Al(100 nm) and measured under AM 1.5 simulated solar light. The polymer solutions were prepared from the metallo-dendritic complexes mixed with

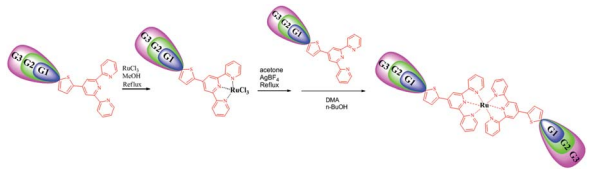

Scheme 2 Synthesis of the single metal system.

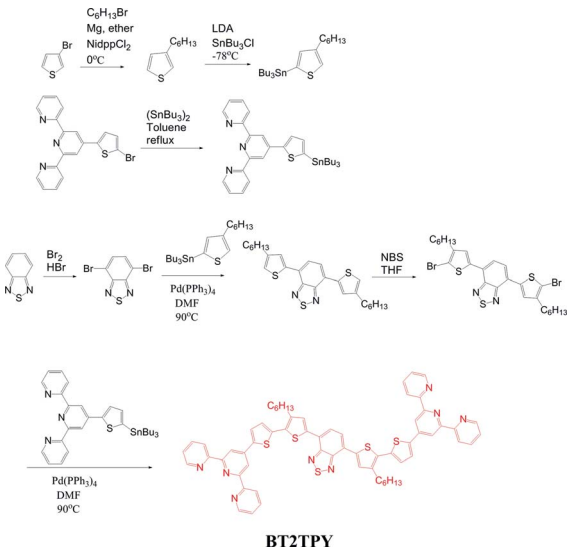

Scheme 3 Synthesis of the core ligand of the double metal system (BT2TPY).

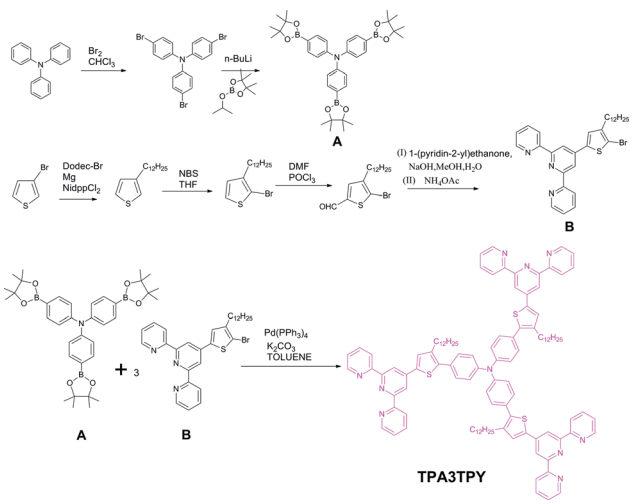

Scheme 4 Synthesis of the core ligand of the triple metal system (TPA3TPY).

$PC_{70}BM$ in chloroform. The current density (J) *versus* voltage (V) curves for the PVCs are demonstrated in Fig. 9, where the open circuit voltage (V_{oc}), short circuit current density (J_{sc}), fill factor (FF) and power conversion efficiency (PCE) values are summarized in Table 3. According to the theory, V_{oc} values should depend on the difference between the HOMO levels of the

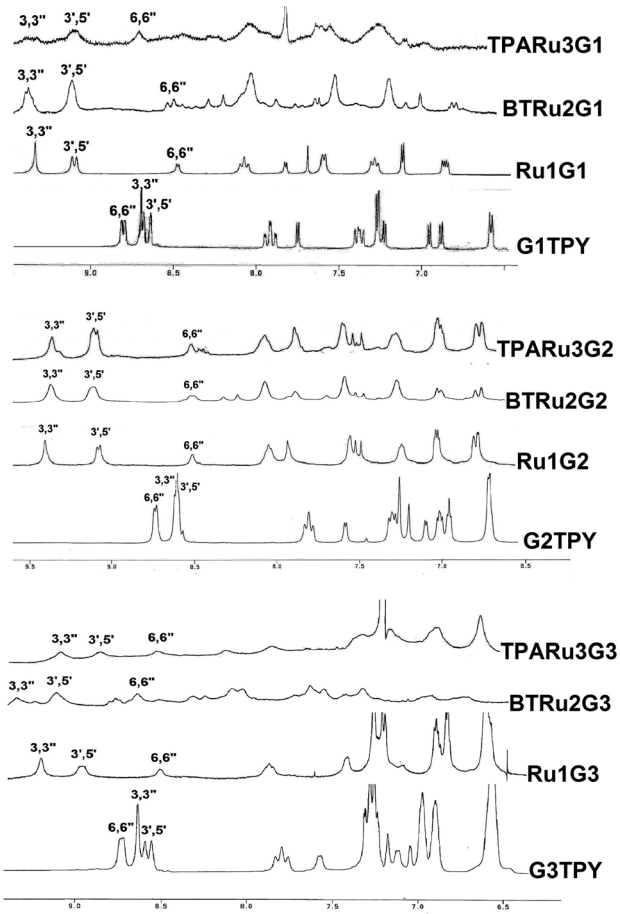

Fig. 5 NMR characterization for the formation of the Ru core.

electron donors (*i.e.*, metallo-dendrimers) and the LUMO level of the electron acceptor (*i.e.*, **$PC_{70}BM$**). However, several other parameters would also critically affect the usual trend in the V_{oc}

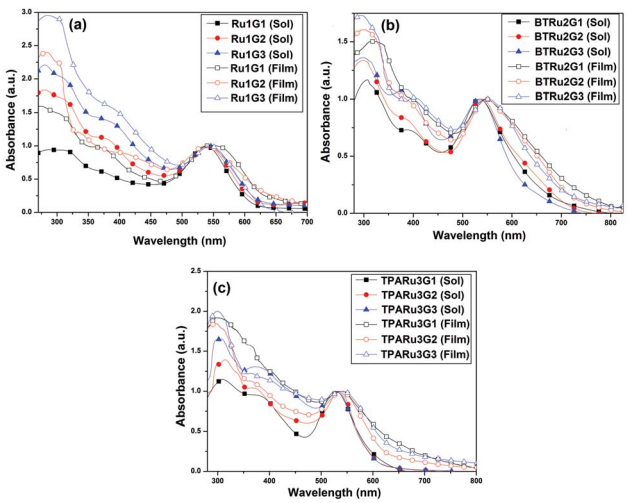

Fig. 6 UV-Vis absorption spectra of the supramolecular dendritic metal complexes in CHCl3 at $c = 1 \times 10^{-5}$ M (solid symbols) and solid films (hollow symbols). (a) mono-, (b) bis- and (c) tris-Ru-based systems.

Table 1 Optical properties of Ru-based dendritic complexes

Dendritic complex	$\lambda_{abs,sol}$ [a] [nm]	$\lambda_{abs,film}$ [b] [nm]	λ_{onset} [nm]	E_g^{optc} [eV]	τ_{avg} [d] [ns]
Ru1G1	537	552	665	1.86	6.136
Ru1G2	541	543	683	1.81	4.112
Ru1G3	545	547	691	1.79	3.021
BTRu2G1	534	545	786	1.57	2.351
BTRu2G2	537	550	797	1.55	2.039
BTRu2G3	540	553	816	1.51	1.604
TPARu3G1	526	536	711	1.74	2.972
TPARu3G2	533	541	750	1.65	2.505
TPARu3G3	535	545	772	1.60	2.003

[a] Concentration of 10^{-5} M in chloroform solutions. [b] Spin-coated from the solutions on quartz substrates. [c] Optical band gaps were estimated from the absorption spectra in films using the equation $E_g = 1240/\lambda_{edge}$. [d] Time-resolved fluorescence lifetime.

Table 2 Energy levels and bandgaps of the Ru-based dendritic complexes[a]

Dendritic complex	E_{red} [b] [V]	LUMO[c] [eV]	E_{ox} [b] [V]	HOMO[c] [eV]	E_g^{el} [eV]
Ru1G1	−0.59	−3.75	0.92	−5.27	1.52
Ru1G2	−0.61	−3.74	0.89	−5.24	1.50
Ru1G3	−0.71	−3.64	0.82	−5.17	1.53
BTRu2G1	−0.69	−3.65	0.82	−5.17	1.52
BTRu2G2	−0.70	−3.64	0.79	−5.14	1.50
BTRu2G3	−0.72	−3.62	0.77	−5.12	1.50
TPARu3G1	−0.69	−3.65	0.86	−5.21	1.56
TPARu3G2	−0.71	−3.63	0.81	−5.16	1.53
TPARu3G3	−0.72	−3.62	0.80	−5.15	1.53

[a] Reduction and oxidation potentials measured by cyclic voltammetry in solid films. [b] Onset oxidation and reduction potentials. [c] $E_{HOMO/ELUMO} = [-(E_{onset} - 0.45) - 4.8]$ eV, where 0.45 V is the value for ferrocene *vs.* Ag/Ag+ and 4.8 eV is the energy level of ferrocene below the vacuum.

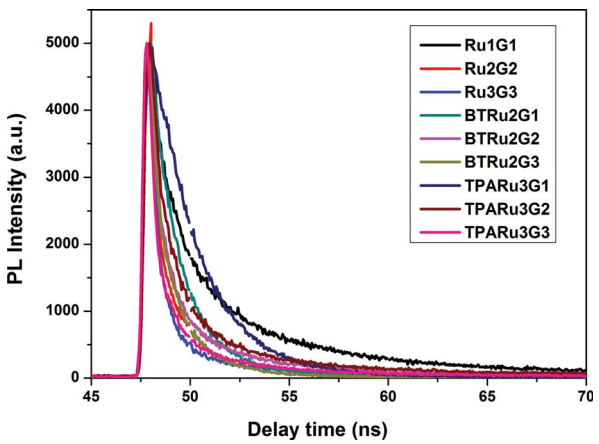

Fig. 7 Time-resolved fluorescence spectra of the supramolecular Ru-based dendritic complexes.

values, such as the carrier recombination, the resistance related to the thickness of the active layer and the degree of phase separation between the different components in the polymer blend, which could energetically amend the expected V_{oc} values. Therefore, according to the higher generation of the metallo-dendrimers their HOMO levels were sequentially enhanced, but their corresponding V_{oc} values also increased.[8m–q] This result might be related to the higher efficiency of the electron transfer (possessing a shorter life time of PL) induced by the increased electron donor thiophene moieties in the metallo-dendrimers with higher generations. Compared with the single and triple metal systems, the higher efficiencies of the double metal system could be attributed to the presence of the dendritic thiophene arms and bis-Ru-based core ligand (as electron donor and acceptor moieties, respectively) to induce stronger ICT bands and broader sensitization ranges. According to the

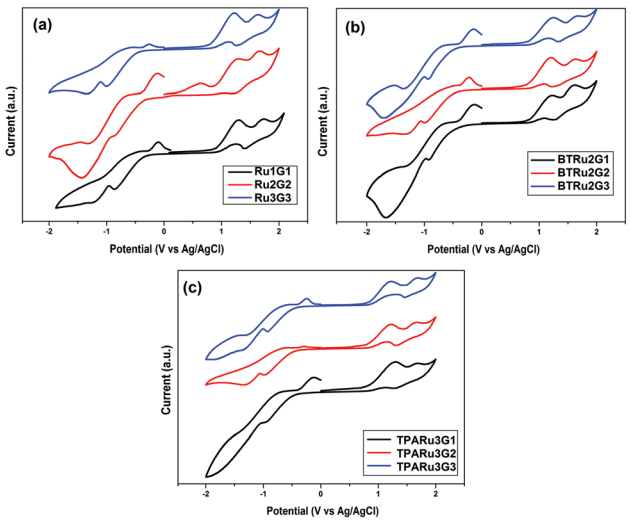

Fig. 8 CV spectra of Ru-based dendritic complexes in solid films. (a) mono-, (b) bis- and (c) tris-Ru-based systems.

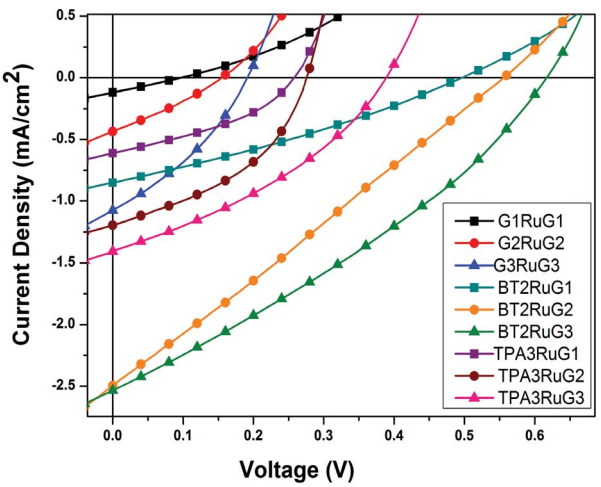

Fig. 9 Current density–voltage curves of the BHJ solar cells using blended films of "mono-, bis-, tris-Ru(II)-based metallo-dendritic complexes": $PC_{70}BM$ 1 : 1 (w/w) under the illumination of AM 1.5 G, 100 mW cm^{-2}.

Table 3 Photovoltaic properties of BHJ solar cell devices with a configuration of ITO/PEDOT:PSS/dendritic complex:$PC_{70}BM$ = 1 : 1 (w/w)/Ca/Al[a]

Active layer[b] dendritic complex:$PC_{70}BM$ (1 : 1 w/w)	V_{oc} [V]	J_{sc} [mA cm^{-2}]	FF [%]	PCE [%]
Ru1G1	0.10	0.12	25.0	0.003
Ru1G2	0.16	0.44	28.01	0.02
Ru1G3	0.20	1.07	32.4	0.07
BTRu2G1	0.49	0.84	33.78	0.14
BTRu2G2	0.55	2.49	26.34	0.36
BTRu2G3	0.61	2.54	32.67	0.51
TPARu3G1	0.26	0.61	37.83	0.06
TPARu3G2	0.28	1.20	41.66	0.14
TPARu3G3	0.39	1.40	34.79	0.19

[a] Measured under AM 1.5 irradiation, 100 mW cm^{-2}. [b] Active layer with the weight ratio of dendritic complex: $PC_{70}BM$ = 1 : 1.

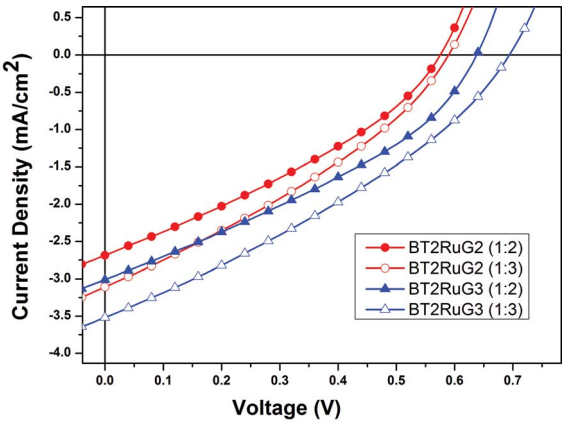

Fig. 10 Current density–voltage curves of the BHJ solar cells using an active layer of BTRu2G2 and BTRu2G3 blended with $PC_{70}BM$ in two different weight ratios (1 : 2 & 1 : 3) under the illumination of AM 1.5G, 100 mW cm^{-2}.

above photovoltaic results, the BHJ PSC device containing an active layer of **BTRu2G3 : $PC_{70}BM$** = 1 : 1 (w/w) revealed the best PCE value of 0.51, which is consistent with the shortest fluorescence life time of **BTRu2G3** (in Table 1) among all the metallo-dendritic complexes. Tris-Ru-based architectures with the terthiophene-triphenylamine core ligand showed moderate photovoltaic performance due to their star-shaped branched

Table 4 Photovoltaic properties of the BHJ solar cell devices with a configuration of ITO/PEDOT:PSS/dendritic complex:PC70BM/Ca/Al[a]

Active layer dendritic complex:$PC_{70}BM$	V_{oc} [V]	J_{sc} [mA cm^{-2}]	FF [%]	PCE [%]
BTRu2G2 : $PC_{70}BM$ = 1 : 2 (w/w)	0.57	2.69	32.97	0.50
BTRu2G2 : $PC_{70}BM$ = 1 : 3 (w/w)	0.59	3.11	32.41	0.59
BTRu2G3 : $PC_{70}BM$ = 1 : 2 (w/w)	0.63	3.02	34.77	0.66
BTRu2G3 : $PC_{70}BM$ = 1 : 3 (w/w)	0.69	3.51	31.89	0.77

[a] Measured under AM 1.5 irradiation, 100 mW cm^{-2}.

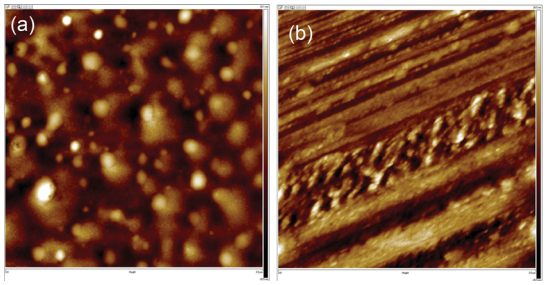

Fig. 11 AFM images of blended (a) BTRu2G2 : $PC_{70}BM$ and (b) BTRu2G3 : $PC_{70}BM$ spin-coated from chloroform in the ratio of 1 : 3 (w/w).

structures possessing an electron deficient acceptor moiety in the core ligand.

The two best photovoltaic performances of the BHJ PSC cells containing bis-Ru(II)-based dendritic complexes, *i.e.*, **BTRu2G2** and **BTRu2G3**, were further optimized by fabricating the active layer using different weight ratios (*i.e.*, 1 : 2 and 1 : 3 w/w) of **BTRu2G2 : $PC_{70}BM$** and **BTRu2G3 : $PC_{70}BM$**. The J–V curves of the PSC devices are shown in Fig. 10 and their related photovoltaic data listed in Table 4. The best PCE value of 0.77% with V_{oc} = 0.69 V, J_{sc} = 3.51 mA cm^{-2} and FF = 31.89% was obtained in the PSC device containing **BTRu2G3 : $PC_{70}BM$** = 1 : 3 (w/w).

Fig. 11 represents the atomic force microscopic (AFM) images of **BTRu2G2 : $PC_{70}BM$** (1 : 3) and **BTRu2G3 : $PC_{70}BM$** (1 : 3), and the root mean square roughnesses (R_{rms}) of these images were found to be 8.0 nm and 7.3 nm, respectively. The higher roughness could reduce the charge-transport distance and at the same time provide a nano-scaled texture that further enhances internal light scattering and light absorption. However, the J_{sc} value was decreased in **BTRu2G2 : $PC_{70}BM$** (1 : 3) compared with **BTRu2G3 : $PC_{70}BM$** (1 : 3). This is due to the larger R_{rms} of **BTRu2G2 : $PC_{70}BM$** (1 : 3) compared to **BTRu2G3 : $PC_{70}BM$** (1 : 3), causing large-scaled phase separation, which decreased the diffusional escape probabilities for the mobile charge carriers,; hence, the charge recombination increased, which is consistent with J_{sc} and PCE values obtained.

Conclusions

Herein, we have synthesized three series of mono-, bis- and tris-Ru-based supramolecular dendritic metal complexes. Their suitable photophysical and electrochemical properties, such as extended absorption ranges and lower optical as well as electrochemical bandgaps, revealed these metallo-dendritic complexes to be useful for photovoltaic applications. Tris-Ru-based complexes with a terthiophene-triphenylamine core showed moderate photovoltaic performance possibly originating from the non-planar structure of each dendritic branch that causes hindered electron transport. Compared with the other two series (mono- and tris-Ru-based dendritic metal complexes), bis-Ru-based dendritic complexes possessed higher PCE values due to the proper molecular design of the donor–acceptor architecture, containing a benzothiadiazole-hexyl

thiophene core as an electron acceptor moiety. Among the three generations (G1–G3) of all the supramolecular complexes, larger PCE values were obtained in the higher generations of the metallo-dendritic complexes in each individual mono-, bis- and tris-'Ru'-based series. Therefore, the PSC device containing an active layer of **BTRu2G3 : $PC_{70}BM$** = 1 : 3 (w/w) (*i.e.*, the third generation of the bis-Ru-based dendritic complex **BTRu2G3**) showed the highest PCE value of 0.77%. Compared with our previous report on main-chain Ru(II) metallo-polymers (containing bi-thiophene linkers and benzothiadiazole acceptor) with PCE = 0.45%,[4m] a higher power conversion efficiency (PCE = 0.77%) could be obtained by taking a similar benzothiadiazole acceptor and thiophene dendrons in the monodisperse system of **BTRu2G3**. However, the photovoltaic efficiency could be further improved by suitable and selective incorporations of dendritic analogues with higher fill factors (improved film qualities) and enhanced short circuit current densities.

Acknowledgements

The financial support of this project was provided by the National Science Council of Taiwan ROC) through NSC 101-2113-M-009-013-MY2 and NSC102-2221-E-009-174 and National Chiao Tung University through 97W807.

References

1 (*a*) H. Choi, M. Kuno, G. V. Hartland and P. V. Kamat, *J. Mater. Chem. A.*, 2013, **1**, 5487; (*b*) Z. Mu, Q. Shao, J. Ye, Z. Zeng, Y. Zhao, H. H. Hng, F. Y. C. Boey, J. Wu and X. Chen, *Langmuir*, 2011, **27**, 1314; (*c*) K. E. Erkkila, D. T. Odom and J. K. Barton, *Chem. Rev.*, 1999, **99**, 2777; (*d*) I. V. Lightcap and P. V. Kamat, *Acc. Chem. Res.*, 2013, **46**, 2235; (*e*) F. Barigelletti and L. Flamigni, *Chem. Soc. Rev.*, 2000, **29**, 1; (*f*) P. Lainé, F. Bedioui, E. Amouyal, V. Albin and F. Burruyer-Penaud, *Chem.–Eur. J.*, 2002, **8**, 3162; (*g*) S. Ott, M. Kritikos, B. Akermark and L. Sun, *Angew. Chem., Int. Ed.*, 2003, **42**, 3285; (*h*) P. R. Andres and U. S. Schubert, *Adv. Mater.*, 2004, **16**, 1043; (*i*) N. K. Subbaiyyan, I. Obraztsov, C. A. Wijesinghe, K. Tran, W. Kutner and F. D'Souza, *J. Phys. Chem. C*, 2009, **113**, 8982; (*j*) H. Hofmeier and U. S. Schubert, *Chem. Soc. Rev.*, 2004, **33**, 373; (*k*) G. Bianké and R. Häner, *ChemBioChem*, 2004, **5**, 1063; (*l*) M. Schmittel, V. Kalsani, R. S. K. Kishore, H. Colfen and J. W. Bats, *J. Am. Chem. Soc.*, 2005, **127**, 11544; (*m*) M. Schmittel, V. Kalsani, P. Mal and J. W. Bats, *Inorg. Chem.*, 2006, **45**, 6370; (*n*) S. H. Hwang, C. N. Moorefield, L. Dai and G. R. Newkome, *Chem. Mater.*, 2006, **18**, 4019; (*o*) E. Maligaspe, A. S. D. Sandanayaka, T. Hasobe, O. Ito and F. D'Souza, *J. Am. Chem. Soc.*, 2010, **132**, 8158.

2 (*a*) J.-F. Gohy, B. G. G. Lohmeijer and U. S. Schubert, *Chem.–Eur. J.*, 2003, **9**, 3472; (*b*) E. Puodziukynaite, L. Wang, K. S. Schanze, J. M. Papanikolas and J. R. Reynolds, *Polym. Chem.*, 2014, **5**, 2363; (*c*) K. Feng, X. Shen, Y. Li, Y. He, D. Huang and Q. Peng, *Polym. Chem.*, 2013, **4**, 5701.

3 (*a*) A. S. A. E. Aziz, J. L. Pilfold, B. Z. Momeni, A. J. Prouda and J. K. Pearson, *Polym. Chem.*, 2014, **5**, 3453; (*b*) J.-M. Lehn, *Supramolecular Chemistry, Concept and Perspectives*, VCH, Weinheim, 1995; (*c*) G. R. Newkome, E. He and C. N. Moorefield, *Chem. Rev.*, 1999, **99**, 1689; (*d*) U. S. Schubert and C. Eschbaumer, *Angew. Chem., Int. Ed.*, 2002, **41**, 2892; (*e*) G. R. Newkome, P. Wang, C. Moorefield, T. J. Cho, P. P. Mohapatra, S. Li, S. H. Hwang, O. Lukoyanova, L. Echegoyen, J. A. Palagallo, V. Lancu and S.-W. Hla, *Science*, 2006, **312**, 1782; (*f*) S. Basak, Y. S. L. V. Narayana, M. Baumgarten, K. Müllen and R. Chandrasekar, *Macromolecules*, 2013, **46**, 362; (*g*) S. Flores-Torres, G. R. Hutchison, L. J. Soltzberg and H. D. Abruña, *J. Am. Chem. Soc.*, 2006, **128**, 1513; (*h*) S. Bonnet, J. P. Collin, M. Koizumi, P. Mobian and J. P. Sauvage, *Adv. Mater.*, 2006, **18**, 1239.

4 (*a*) K. W. Cheng, C. S. C. Mak, W. K. Chan, A. M. C. Ng and A. B. Djurii, *J. Polym. Sci., Part A: Polym. Chem.*, 2008, **46**, 1305; (*b*) K. K. Y. Man, H. L. Wong, W. K. Chan, C. Y. Kwong and A. B. Djurisic, *Chem. Mater.*, 2004, **16**, 365; (*c*) P. D. Vellis, J. A. Mikroyannidis, C. N. Lo and C. S. Hsu, *J. Polym. Sci., Part A: Polym. Chem.*, 2008, **46**, 7702; (*d*) V. Duprez, M. Biancardo, H. Spanggaard and F. C. Krebs, *Macromolecules*, 2005, **38**, 10436; (*e*) O. Hagemann, M. Jørgensen and F. C. Krebs, *J. Org. Chem.*, 2006, **71**, 5546; (*f*) K. K. Y. Man, H. L. Wong, W. K. Chan, A. B. Djurisic, E. Beach and S. Rozeveld, *Langmuir*, 2006, **22**, 3368; (*g*) Y. Pan, B. Tong, J. Shi, W. Zhao, J. Shen, J. Zhi and Y. Dong, *J. Phys. Chem. C*, 2010, **114**, 8040; (*h*) V. Stepanenko, M. Stocker, P. Muller, M. Buchner and F. Wurthner, *J. Mater. Chem.*, 2009, **19**, 6816; (*i*) Y. Y. Chen, Y. T. Tao and H. C. Lin, *Macromolecules*, 2006, **39**, 8559; (*j*) W. S. Huang, Y. H. Wu, H. C. Lin and J. T. Lin, *Polym. Chem.*, 2010, **1**, 494; (*k*) J. F. Yin, D. Bhattacharya, Y. C. Hsu, C. C. Tsai, K. L. Lu, H. C. Lin, J. G. Chen and K. C. Ho, *J. Mater. Chem.*, 2009, **19**, 7036; (*l*) J. F. Yin, J. G. Chen, Z. Z. Lu, K. C. Ho, H. C. Lin and K. L. Lu, *Chem. Mater.*, 2010, **22**, 4392; (*m*) H. Padhy, D. Sahu, I. H. Chiang, D. Patra, D. Kekuda, C. W. Chu and H. C. Lin, *J. Mater. Chem.*, 2011, **21**, 1196; (*n*) J. F. Yin, J. G. Chen, J. T. Lin, D. Bhattacharya, Y. C. Hsu, H. C. Lin, K. C. Ho and K. L. Lu, *J. Mater. Chem.*, 2012, **22**, 130.

5 (*a*) P. D. Vellis, J. A. Mikroyannidis, C. N. Lo and C. S. Hsu, *J. Polym. Sci., Part A: Polym. Chem.*, 2008, **46**, 7702; (*b*) H. Padhy, D. Sahu, I. H. Chiang, D. Patra, D. Kekuda, C. W. Chu and H. C. Lin, *J. Mater. Chem.*, 2011, **21**, 1196; (*c*) H. Padhy, M. Ramesh, D. Patra, R. Satapathy, M. K. Pola, H. C. Chu, C. W. Chu, K. H. Wei and H. C. Lin, *Macromol. Rapid Commun.*, 2012, **33**, 528; (*d*) N. K. Subbaiyan, C. A. Wijesinghe and F. D'Souza, *J. Am. Chem. Soc.*, 2009, **131**, 14646; (*e*) S. Deng, G. Krueger, P. Taranekar, S. Sriwichai, R. Zong, R. Thummel and R. Advincula, *Chem. Mater.*, 2011, **23**, 3302; (*f*) S. Caramori, J. Husson, M. Beley, C. A. Bignozzi, R. Argazzi and P. C. Gros, *Chem.–Eur. J.*, 2010, **16**, 2611.

6 (*a*) R. J. Kline, M. D. McGehee, E. N. Kadnikova, J. S. Liu and J. M. J. Fréch, *Adv. Mater.*, 2003, **15**, 1519; (*b*) P. Schilinsky, U. Asawapirom, U. Scherf, M. Biele and C. J. Brabec, *Chem. Mater.*, 2005, **17**, 2175; (*c*) X. N. Yang, J. Loos, S. C. Veenstra, W. J. H. Verhees, M. M. Wienk, J. M. Kroon,

M. A. J. Michels and R. A. J. Janssen, *Nano Lett.*, 2005, **5**, 579; (*d*) N. Kopidakis, W. J. Mitchell, J. Van-de-Lagemaat, D. S. Ginley, G. Rumbles, S. E. Shaheen and W. L. Rance, *Appl. Phys. Lett.*, 2006, **89**, 103524; (*e*) A. M. Nardes, A. J. Ferguson, J. B. Whitaker, B. W. Larson, R. E. Larsen, K. Maturova, P. A. Graf, O. V. Boltalina, S. H. Strauss and N. Kopidakis, *Adv. Funct. Mater.*, 2012, **22**, 5900; (*f*) E. Maligaspe, A. S. D. Sandanayaka, T. Hasobe, O. Ito and F. D'Souza, *J. Am. Chem. Soc.*, 2010, **132**, 8158; (*g*) M. I. Mangione and R. A. Spanevello, *Macromolecules*, 2013, **46**, 4754; (*h*) K. Chiad, M. Grill, M. Baumgarten, M. Klapper and M. Müllen, *Macromolecules*, 2013, **46**, 3554; (*i*) G. Vamvounis, P. E. Shaw and P. L. Burn, *J. Mater. Chem. C*, 2013, **1**, 1322; (*j*) S. A. Ponomarenko, N. N. Rasulova, Y. N. Luponosov, N. M. Surin, M. I. Buzin, I. Leshchiner, S. M. Peregudova and A. M. Muzafarov, *Macromolecules*, 2012, **45**, 2014; (*k*) O. V. Rud, A. A. Polotsky, T. Gillich, O. V. Borisov, F. A. M. Leermakers, M. Textor and T. M. Birshtein, *Macromolecules*, 2013, **46**, 4651; (*l*) C. Q. Ma, E. M. Osteritz, M. Wunderlin, G. Schulz and P. Bauerle, *Chem.–Eur. J.*, 2012, **18**, 12880; (*m*) K. Mutkins, S. S. Y. Chen, A. Pivrikas, M. Aljada, P. L. Burn, P. Meredith and B. J. Powell, *Polym. Chem.*, 2013, **4**, 916; (*n*) J. You, G. Li and Z. Wang, *Polymer*, 2012, **53**, 5116; (*o*) H. Ye, D. Chen, M. Liu, X. Zhou, S. J. Su and Y. Cao, *Polymer*, 2013, **54**, 162.

7 (*a*) T. Hasobe, Y. Kashiwagi, M. A. Absalom, J. Sly, K. Hosomizu, M. J. Crossley, H. Imahori, P. V. Kamat and S. Fukuzumi, *Adv. Mater.*, 2004, **16**, 975; (*b*) R. Bettignies, Y. Nicolas, P. Blanchard, E. Levillain, J. M. Nunzi and J. Roncali, *Adv. Mater.*, 2003, **15**, 1939; (*c*) N. Satoh, T. Nakashima and K. Yamamoto, *J. Am. Chem. Soc.*, 2005, **127**, 13030; (*d*) T. Kengthanomma, P. Thamyongkit, J. Gasiorowski, A. M. Ramil and N. S. Sariciftci, *J. Mater. Chem. A*, 2013, **1**, 10524; (*e*) M. J. Cho, J. Seo, K. Luo, K. H. Kim, D. H. Choi and P. N. Prasad, *Polymer*, 2012, **53**, 3835.

8 (*a*) G. R. Newkome, C. N. Moorefield and F. Vögtle, *Dendrimers and dendrons: concepts, syntheses, applications*, Wiley-VCH, Weinheim, 2001; (*b*) J. M. J. Fréchet and D. A. Tomalia, *Dendrimers and other dendritic polymers*, Wiley, Chi-chester, 2002; (*c*) M. Kawa and J. M. J. Fréchet, *Chem. Mater.*, 1998, **10**, 286; (*d*) C. J. Hawker and J. M. J. Fréchet, *J. Am. Chem. Soc.*, 1992, **114**, 8405; (*e*) V. Maraval, R. Laurent, B. Donnadieu, M. Mauzac, A. M. Caminade and J. P. Majoral, *J. Am. Chem. Soc.*, 2000, **122**, 2499; (*f*) C. Xia, X. Fan, J. Locklin and R. C. Advincula, *Org. Lett.*, 2002, **4**, 2067; (*g*) W. J. Mitchell, A. J. Ferguson, M. E. Köse, B. L. Rupert, D. S. Ginley, G. Rumbles, S. E. Shaheen and N. Kopidakis, *Chem. Mater.*, 2009, **21**, 287; (*h*) A. C. Kanarr, B. L. Rupert, S. Hammond, J. van-de-Lagemaat, J. C. Johnson and A. Ferguson, *J. Phys. Chem. A*, 2011, **115**, 2515; (*i*) J. Cremer and P. Bauerle, *J. Mater. Chem.*, 2006, **16**, 874; (*j*) S. Deng, T. M. Fulghum, G. Krueger, D. Patton, J. Y. Park and R. C. Advincula, *Chem.–Eur. J.*, 2011, **17**, 8929; (*k*) A. Mishra, A. M. Osteritz and P. Bäuerle, *Beilstein J. Org. Chem.*, 2013, **9**, 86; (*l*) G. L. Schulz, M. Mastalerz, C. Q. Ma, M. Wienk, R. Janssen and P. Bäuerle, *Macromolecules*, 2013, **46**, 2141; (*m*) Y. Li, H. Li, B. Xu, Z. Li, F. Chen, D. Feng, J. Zhang and W. Tian, *Polymer*, 2010, **5**, 1786; (*n*) H. Chung, T. Narita, J. Yang, P. Kim, M. Takase, M. Iyoda and D. Kim, *Chem.–Eur. J.*, 2013, **19**, 9699; (*o*) V. Tamilavan, M. Song, R. Agneeswari, J.-W. Kang, D.-H. Hwang and M. H. Hyun, *Polymer*, 2013, **54**, 6125; (*p*) E. Kozma, D. Kotowski, F. Bertini, S. Luzzati and M. Catellani, *Polymer*, 2010, **51**, 2264; (*q*) Y. Sun, B. Lin, H. Yang and X. Gong, *Polymer*, 2012, **53**, 1535; (*r*) D. Sahu, C. H. Tsai, H. Y. Wei, K. C. Ho, F. C. Chang and C. W. Chu, *J. Mater. Chem.*, 2012, **22**, 7945; (*s*) J. M. Jiang, H. C. Chen, H. K. Lin, C. M. Yu and S. C. Lan, *Polym. Chem.*, 2013, **4**, 5321; (*t*) S. C. Lan, P. A. Yang, M. J. Zhu, C. M. Yu, J. M. Jiang and K. H. Wei, *Polym. Chem.*, 2013, **4**, 113; (*u*) V. Tamilavan, M. Song, S.-H. Jin and M. H. Hyun, *Polymer*, 2011, **52**, 2384.